Confined diffusion in tubular structures analyzed by fluorescence correlation spectroscopy on a mirror

Emilien Etienne, Pierre-François Lenne, James N. Sturgis, and Hervé Rigneault

In fluorescence correlation spectroscopy (FCS) analysis it is generally assumed that molecular species diffuse freely in volumes much larger than the three-dimensional FCS observation volume. However, this standard assumption is not valid in many measurement conditions, particularly in tubular structures with diameters in the micrometer range, such as those found in living cells (organelles, dendrites) and microfluidic devices (capillaries, reaction chambers). As a result the measured autocorrelation functions (ACFs) deviate from those predicted for free diffusion, and this can shift the measured diffusion coefficient by as much as ~50% when the tube diameter is comparable with the axial extension of the FCS observation volume. We show that the range of validity of the FCS measurements can be drastically improved if the tubular structures are located in the close vicinity of a mirror on which FCS is performed. In this case a new fluctuation time in the ACF, arising from the diffusion of fluorescent probes in optical fringes, permits measurement of the real diffusion coefficient within the tubular structure without assumptions about either the confined geometry or the FCS observation volume geometry. We show that such a measurement can be done when the tubular structure contains at least one pair of dark and bright fringes resulting from interference between the incoming and the reflected excitation beams on the mirror surface. Measurement of the diffusion coefficient of the enhanced green fluorescent protein (EGFP) and IscS-EGFP in the cytoplasm of living *Escherichia coli* illustrates the capabilities of the technique.

OCIS codes: 300.2530, 300.6280, 120.2650, 120.3930, 170.6280, 170.1420.

1. Introduction

The analysis of the temporal fluctuations of fluorescence light coming from molecular emitters is nowadays a well-established method for obtaining information about thermodynamic and kinetic processes at the single-molecule level. The most common approach, namely, fluorescence correlation spectroscopy (FCS), was introduced in the early 1970s[1–3] and is used to analyze the spontaneous signal fluctuations that occur at a microscopic scale in a system of fluorescent molecules. In practice, fluctuation analysis is possible if the system under observation is restricted to very small ensembles of molecular emitters and the collected fluorescence in discriminated against the background. This is usually accomplished by combining low sample concentration (picomolar to nanomolar) with a small observation volume (~0.3 femtoliter). This observation volume, which is restricted by the diffraction limit of microscope objective lenses with high numerical aperture,[4] can be considered approximately as a three-dimensional Gaussian volume. Although this Gaussian assumption proved to have some limitations,[5] it is commonly used in biological applications[6–9] and microfluidics.[10] In FCS the fluctuations are analyzed by temporally autocorrelating the recorded photocount signal and quantified by the fluctuation autocorrelation function (ACF). The ACF is a function of the time delay τ and can concretely be related to the probability of collecting a photon at time $t + \tau$, if a photon was collected at time t. Although one can always build such a function, its interpretation requires precise knowledge of (1) the shape of the FCS observation volume, (2) the diffusion statistics, and (3) the boundary conditions. In standard FCS a three-dimensional Gaussian observation volume and Brownian diffu-

E. Etienne, P.-F. Lenne (e-mail, lenne@fresnel.fr), and H. Rigneault (e-mail, herve.rigneault@fresnel.fr) are with the Institut Fresnel, Mosaic Group, Unité Mixte de Recherche, Centre National de la Recherche Scientifique 6133, Université Paul Cézanne Aix-Marseille III, Domaine Universitaire de St-Jérôme, 13397 Marseille Cedex 20, France. J. N. Sturgis is with Institut de Biologie Structurale et Microbiologie, IFR 88, Laboratoire d'Ingénierie des Systèmes Macromoléculaires, UPR 9027, 31 Chemin Joseph Aiguier, 13402 Marseille Cedex 20, France.

Received 19 October 2005; revised 12 January 2006; accepted 18 January 2006; posted 24 January 2006 (Doc. ID 65465).

0003-6935/06/184497-11$15.00/0

sion in an infinite diffusion volume are usually considered.[11] These assumptions lead to a theoretical expression of the ACF that is then fitted to the experimental ACF, yielding, as adjusted parameters, to the average number N of fluorescent molecules in the observation volume and the diffusional residence time τ_D, which can be used to find the diffusion coefficient D, if the dimensions of the Gaussian volume are known. Nevertheless Gennerich and Schild[12] have shown that the use of the standard FCS model leads to erroneous results when FCS measurements are carried out in small tubular structures, such as neuronal dendrites, or more generally in processes that confine the diffusing particles in structures smaller than the observation volume. Analytical solutions for the ACFs can be found for some simple tubular confinement geometries,[12] but their use in fitting experimental data requires *a priori* knowledge of tube size and geometry.

We report here on the use of FCS on a mirror for studying confined diffusion in tubular structures. This technique enables a structuring of the observation volume,[13–15] which avoids the use of a complex analytical solution for interpretation and needs only a three-free-parameter fitting process. We first show numerically that this technique can be applied to perform measurements in the tubular structure down to a confinement diameter of $\lambda/2$, where λ is the excitation wavelength, whereas standard FCS proves to be accurate for diameters 10 times larger. Then we illustrate the capabilities of this technique by measuring the diffusion coefficient of two fluorescent proteins [the enhanced green fluorescent protein (EGFP) and IscS-EGFP] in the cytoplasm of *Escherichia coli* (EC).

2. Numerical Study

A. Fluorescence Correlation Spectroscopy in Tubular Structures: Limitations of the Standard Analysis

In this section we study how confined diffusion in tubular structures modifies ACFs and may lead to erroneous measurements when standard FCS analysis is applied. To achieve this task, numerical calculations are implemented to simulate an ACF resulting from the three-dimensional (3D) diffusion of fluorophores confined to a tubular structure. This tubular structure is supposed to be a closed tube lying on the *Oxy* plane, where *O* is the projection of the tube center on *Oxy*. Its diameter is set to $d = 1\ \mu\text{m}$, whereas its length is set to be 3 μm.

We assume that fluorescent particles are independently diffusing in three dimensions, so that we can consider only one fluorescent particle diffusing for a long time in the tube, with a diffusion coefficient set to $D_{\text{simul}} = 10\ \mu\text{m}^2/\text{s}$. Its position x, y, z is randomly calculated at each step of the simulation and is constrained to stay in the tube. When the particle hits the boundaries of the tube, we assume it reflects from the tube. Moreover we assume that a fluorescent particle does not generate any fluorescence fluctuation related to photophysical phenomena.[16] Noise is also omitted.

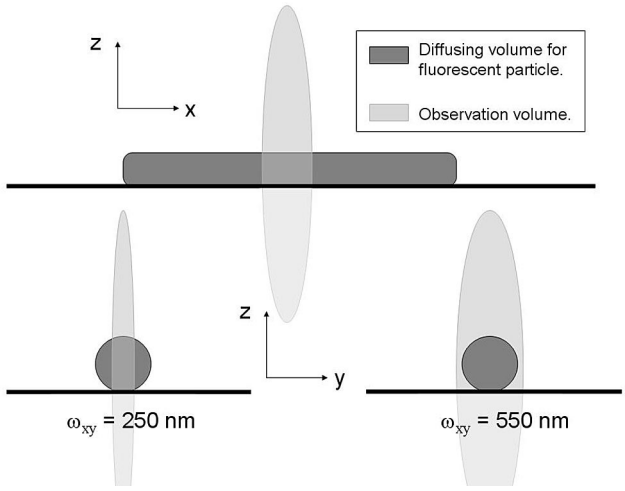

Fig. 1. Spatial configurations for standard FCS for the diffusion coefficient measurement simulation in a tubular structure of diameter $d = 1\ \mu$m (with examples of transversal waist $\omega_{xy} = 250$ nm and $\omega_{xy} = 550$ nm).

For each particle position we calculate the molecular detection efficiency function (MDE), first introduced by Rigler *et al.*[4] This function is related to the detected intensity coming from x, y, z and defines the detection volume. By definition the MDE is the product of the photon flux density profile of the excitation beam and the fluorescence collection efficiency profile of the detection optics. Assuming a 3D Gaussian approximation of the detectable emission intensity distribution, we consider a normalized MDE given by[4]

$$\text{MDE}(x, y, z) = \exp\left(-2\,\frac{x^2+y^2}{\omega_{xy}^{\,2}}\right)\exp\left(-2\,\frac{z^2}{\omega_z^{\,2}}\right), \quad (1)$$

where ω_{xy} and ω_z are, respectively, the transverse and the axial waists, at which the intensity of the laser beam has dropped by $1/e^2$. The structure parameter s, defined as $s = \omega_{xy}/\omega_z$, is set to be 0.2 in the following.

Considering Poissonian emission statistics, the number of emitted and collected photons is calculated along the particle trajectory, yielding to a temporal fluorescence signal. This signal is treated in real time by a numerical correlator.[17] We generated ACFs for transversal waists ω_{xy} ranging between 250 and 550 nm, which are commonly found in experiments. Figure 1 shows the spatial extension of both the observation volume and the tube geometry.

All the resulting ACFs are then fitted by three different theoretical expressions, all based on Brownian diffusion models:

- 3D diffusion (free diffusion along *Ox*, *Oy*, and *Oz*),
- Two-dimensional (2D) diffusion in the *Oxy* plane (free diffusion along *Ox* and *Oy*).

- One-dimensional (1D) free diffusion along Ox.

The general fit formulation of the ACF is given by[11]

$$g^{(2)}(\tau) = 1 + \frac{1}{N} g_x(\tau) g_y(\tau) g_z(\tau), \tag{2}$$

where τ is the delay between two photocounts and N is the average number of fluorescent particles in the detection volume; $g_x(\tau)$, $g_y(\tau)$, and $g_z(\tau)$ are related to diffusion along Ox, Oy, and Oz, respectively. We consider a tubular structure whose extension along Ox is much larger than ω_{xy}. In this case the diffusion is considered as free along this axis and $g_x(\tau)$ is

$$g_x(\tau) = (1 + \tau/\tau_d)^{-1/2}, \tag{3}$$

where τ_d is the average time that a fluorescent particle needs to pass through the detection volume of transversal extension ω_{xy} in an infinite reservoir. The diffusion coefficient is related to τ_d by

$$D = {\omega_{xy}}^2/4\tau_d. \tag{4}$$

Moreover we have

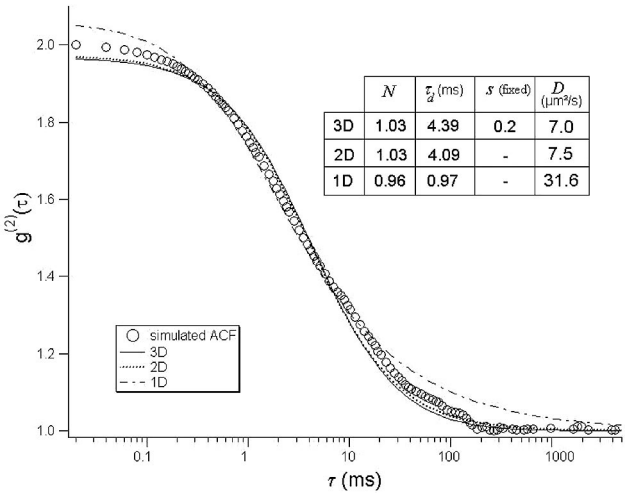

	N	τ_d (ms)	s (fixed)	D (μm²/s)
3D	1.03	4.39	0.2	7.0
2D	1.03	4.09	-	7.5
1D	0.96	0.97	-	31.6

Fig. 2. Simulated ACF (open circles) numerically obtained for a transversal waist, ω_{xy} = 350 nm. The 3D, 2D, and 1D fits are represented with their parameters, s is the structure parameter [see Eq. (6)].

$$g_y(\tau) = \begin{cases} 1 & \text{in the absence of diffusion along } O_y, \\ (1 + \tau/\tau_d)^{-1/2} & \text{for free diffusion along } O_y, \end{cases} \tag{5}$$

$$g_z(\tau) = \begin{cases} 1 & \text{in the absence of diffusion along } O_z, \\ (1 + s^2\,\tau/\tau_d)^{-1/2} & \text{for free diffusion along } O_z, \end{cases} \tag{6}$$

In Fig. 2 is an example of a numerically obtained ACF, the associated fits and fit parameters (ω_{xy} = 350 nm). Note that none of the proposed fits (3D, 2D, and 1D) is satisfactory. Although the fits are not perfect here, diffusion coefficients can be extracted by using Eqs. (2) and (4) with the appropriate expressions of g_x, g_y, and g_z [Eqs. (3), (5), (6)]. Nevertheless the 1D diffusion coefficient (D_{1D} = 31.6 $\mu m^2/s$) is far from the real diffusion coefficient (D_{simul} = 10 $\mu m^2/s$), and this discrepancy remains true for all the considered laser-beam extensions. Therefore we no longer consider the 1D diffusion fit.

In Fig. 3 we present the diffusion coefficients that we obtained from the 3D and 2D fits, when ω_{xy} is varied from 250 to 550 nm. The true diffusion coefficient D_{simul} is represented by the dotted line. Thus diffusion coefficient measurements lead to erroneous results for almost all transversal waists when performed with a standard FCS analysis in the tubular structure. The smaller waist (ω_{xy} = 250 nm) seems to give acceptable measurements, but we will see that a confinement diameter reduction leads also to unacceptable measurements.

B. Fluorescence Correlation Spectroscopy on a Mirror in the Study of Confined Diffusion in Tubular Structures

Previous studies have shown that a mirror placed at the focus of a microscope objective enhances the photocount rate per molecule and produces a patterning of the observation volume thanks to interference fringes.[13–15] We show in this subsection that this patterning enables us to perform accurate measurements of confined diffusion in a tubular structure when the latter is located in the close vicinity of a mirror surface.

We simulate now ACFs resulting from diffusion inside a tube lying on a mirror. In Fig. 4 we present the new spatial configuration. We have demonstrated that when FCS is performed with a focal spot focused on a mirror the MDE can be well approximated by[14,15]

$$\text{MDE}(x, y, z) = \exp\left(-2\,\frac{x^2 + y^2}{{\omega_{xy}}^2}\right)\exp\left(-2\,\frac{z^2}{{\omega_z}^2}\right) \times 2\cos^2\left(\frac{2\pi n_{\text{tube}}}{\lambda_0}\,z\right), \tag{7}$$

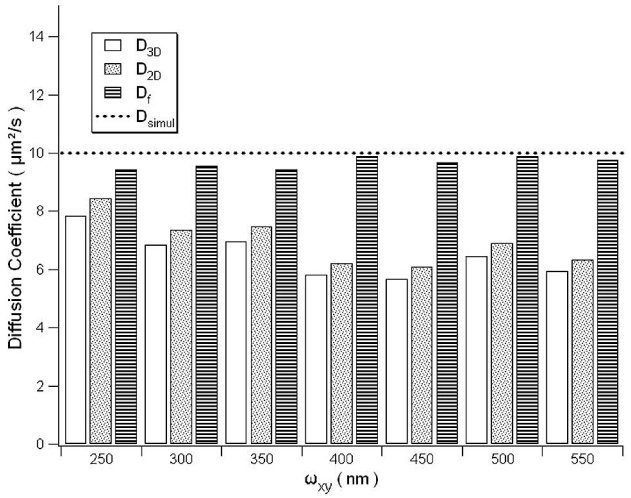

Fig. 3. Diffusion coefficients, obtained from the numerical calculations in a tubular structure with a confinement diameter, d = 1 μm, resulting from standard FCS analysis (D_{3D} and D_{2D}) and from FCS on the mirror with our fringe spacing method (D_f), depending on the transversal waist ω_{xy}. Dotted line, D_{simul} = 10 μm²/s, stands for the diffusion coefficient in the simulations. Whatever the transversal waist the standard FCS analysis leads to an erroneous diffusion coefficient estimation, whereas analysis of FCS on mirror leads to a good measurement.

where n_{tube} is the refractive index in the tube medium and λ_0 is the excitation wavelength. Equation (7) assumes perfectly contrasted fringes with a bright fringe at the surface of the mirror ($z = 0$). In the following we set $n_{tube} = 1.37$ and $\lambda_0 = 488$ nm.

The general fit formula of ACF with the MDE given in Eq. (7), is (details in Appendices A–C)

$$g_M^{(2)}(\tau) = 1 + \frac{1}{N}[1 + n_f \exp(-\tau/\tau_f)]g_x(\tau)g_y(\tau)g_z(\tau), \tag{8}$$

where n_f is a constant (see below and Appendices A–C) and

$$\tau_f = \frac{\lambda^2}{16\pi^2 D} = \frac{{\lambda_0}^2}{16\pi^2 n_{tube} D}. \tag{9}$$

Term τ_f is called the fringe spacing time and is related to the average time that a particle needs to go through a bright or dark fringe (usually $\tau_f < \tau_d$). Note that N is still the average number of fluorescent particles in the detection volume without fringes. Thus, given η_{tube} and λ_0, the measurement of τ_f allows the determination of the diffusion coefficient D.[14] Note that in standard FCS analysis a knowledge of w_{xy} is required [Eq. (4)].

To measure the diffusion coefficient with Eq. (9), ACF_M (ACF obtained on a mirror) should be fitted with Eq. (8) so that the fringe spacing time τ_f is extracted. As derived in Appendices A–C, Eq. (8) is valid for free diffusing species (i.e., no confinement). Following the experimental geometry in Fig. 4, we assume that Eq. (4) remains valid when several fringes are located inside the confined area (tube diameter). In other words, when the fringe spacing is shorter than the confinement extension along the Oz axis, we consider that Eq. (8) is valid. We see below that this assumption proves correct.

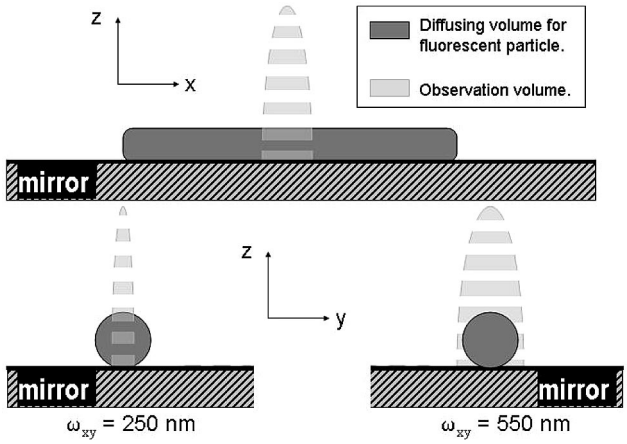

Fig. 4. Spatial configurations of FCS on a mirror for diffusion coefficient measurement simulation in a tubular structure of diameter d = 1 μm lying on a mirror (example of transversal waist ω_{xy} = 250 nm and ω_{xy} = 550 nm). The interference fringes reshape the excitation volume.

On the contrary we make no assumption concerning $g_x(\tau)$, $g_y(\tau)$, and $g_z(\tau)$, which are generally very affected by the confinement (see Fig. 2).

In this framework, and to get rid of the unknown terms $g_x(\tau)$, $g_y(\tau)$, and $g_z(\tau)$, we propose recording ACF both with and without a mirror and calculate for short times ($\tau \leq \tau_d$), $\rho(\tau)$ defined as

$$\rho(\tau) = \frac{ACF_M(\tau) - 1}{ACF_S(\tau) - 1}, \tag{10}$$

where ACF_M and ACF_S account for the ACF obtained in a tubular structure with a mirror and without a mirror (simple surface), respectively. ACF_M and ACF_S are defined by Eqs. (8) and (2), respectively. Generally all the parameters indexed afterward with M or S are related to the case with or without a mirror, respectively. We can suppose without restriction that the diffusion factor $g_x(\tau)g_y(\tau)g_z(\tau)$, which is affected by the confinement, remains the same in Eqs. (2) and (8) since the diffusion mode is similar in these two cases. Therefore $\rho(\tau)$ can be written as

$$\rho(\tau) = A[1 + n_f \exp(-\tau/\tau_f)], \tag{11}$$

where

$$A = N_S/N_M. \tag{12}$$

Even if N_S and N_M stand for the total number of fluorescent molecules in the collection volume without fringes, these parameters are not necessarily equal.

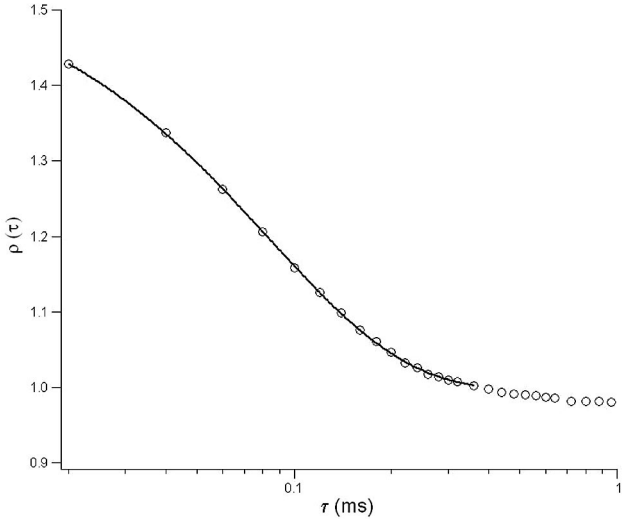

Fig. 5. Simulated ρ function: Circles, ρ ratio calculated from the simulated ACF with and without a mirror; curve, its fit from Eq. (11) for a diffusion in a tubular structure of diameter $d = 1$ μm and for a transversal waist $\omega_{xy} = 400$ nm.

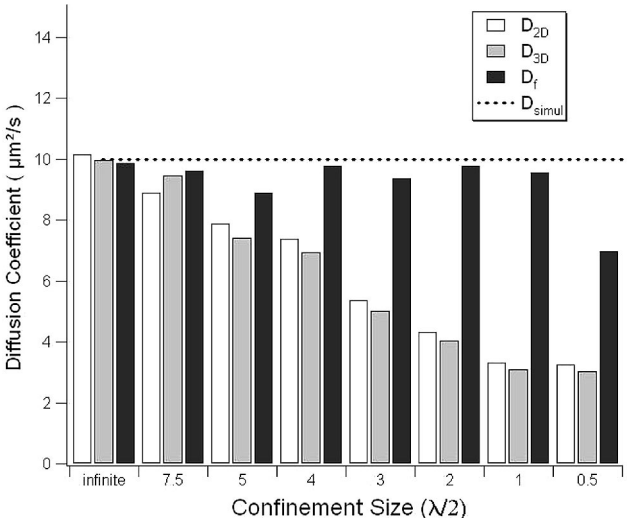

Fig. 6. Diffusion coefficients deduced from various fits: standard FCS analysis with the standard 3D model (D_{3D}) and with the standard 2D model (D_{2D}), and from FCS on a mirror with our fringe spacing method (D_f), depending on the diameter of the confinement tube. Dotted line, $D_{simul} = 10$ μm^2/s, the input diffusion coefficient in the simulations and $\omega_{xy} = 250$ nm.

Compared with Eq. (8), Eq. (11) is easier to fit since only three free parameters are needed. The fringe spacing time τ_f is extracted from Eq. (11) leading to the diffusion coefficient thanks to Eq. (9). Figure 5 gives an example of a simulated ρ function obtained from simulated ACFs and its fit by Eq. (11).

From Fig. 3 one can appreciate how the fringe spacing method that uses Eqs. (9)–(11) can accurately predict the diffusion coefficient D_{simul}.

Moreover Eq. (9) indicates that the fringe spacing time τ_f requires no knowledge of the transversal waist ω_{xy},[14,15] which can be of the order or even larger than the tube diameter.

We determine now the smallest confinement at which FCS on a mirror still gives a correct diffusion coefficient. Figure 6 shows the diffusion coefficients obtained numerically with standard FCS analysis (D_{2D} and D_{3D}) and FCS on a mirror (D_f) when the confinement diameter decreases. (An infinite confinement size means no confinement.) Note that the numerical calculations consider $\omega_{xy} = 0.25$ μm, $n_{tube} = 1.37$, and $\lambda_0 = 488$ nm, hence an excitation wavelength $\lambda = \lambda_0/n_{tube}$. Confinement diameters are given in fringe spacing unit $\lambda/2$, which is the longitudinal size of one couple of bright and dark fringes. A measurement is considered to be valid when it equals D_{simul} within a 10% error; then FCS on a mirror provides acceptable measurements for a confinement diameter larger or equal to $\lambda/2$. On the other hand, standard FCS analysis gives acceptable results for a confinement diameter larger than $10\lambda/2$. Thus, when FCS is used on a mirror, it is possible theoretically to measure a diffusion coefficient (within a 10% error) in structure as small as $\lambda/2$. In other words a sole bright- and dark-fringe pair is sufficient to probe the free diffusion inside the confinement volume.

To conclude this section, Fig. 7 presents a summary of our results. Both analysis range of validity for the FCS on a mirror and for the standard FCS are presented versus the confinement size (in units of $\lambda/2$). In the same medium, with the same excitation wavelength, FCS on a mirror can measure the diffusion coefficient into a confined volume 10 times smaller than standard FCS does.

3. Diffusion Coefficient Measurement in Living *Escherichia Coli* Cytoplasms with Fluorescence Correlation Spectroscopy on a Mirror

To illustrate the capabilities of the technique, we apply our method of FCS on a mirror to perform coefficient diffusion measurements in EC cytoplasms. EC can be considered as a cylinder with a diameter of 1 μm and a length of 5 μm and is filled with a cytoplasm with a refractive index of 1.37.[18]

A. Materials and Methods

1. Mirror

The mirror was designed in our laboratory to reflect both the excitation and the emission wavelengths of the EGFP.[14] This mirror is a (silica substrate)/$(HL)^L$ stack[15] of 16 thin layers, where H and L are the quarter-wavelength layer at 530 nm of the high and the low refractive index, respectively [$n_H = 1.9$ (HfO_2) and $n_L = n_S = 1.5$ (SiO_2)].

To have similar configurations, note that FCS without mirror experiments is performed on a silica substrate (a simple surface).

2. Escherichia Coli Culture and Sample Preparation

All chemicals cited in this subsection were purchased from Sigma-Aldrich (Saint Louis, Mo.). EGFP and IscS-EGFP recombinent proteins were expressed in the EC TG1 strain. The buffer composition is

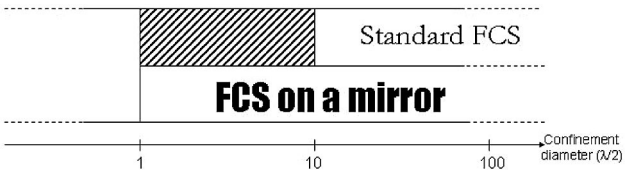

Fig. 7. Range of validity for standard FCS and FCS on a mirror, depending on the confinement diameter expressed in the fringe spacing; λ is the excitation wavelength in the diffusion medium.

- the M9 medium (10×) [Na_2HPO_4 (500 mM), KH_2PO_4 (220 mM), NaCl (85 mM), NH_4Cl (187 mM), pH = 7.2];
- glucose (100×) at 40%;
- ampicilin (250×) at 25 mg/mliter;
- a mix of 16 amino acids (10×) (cystein, asparagin, methionin, and glutamin are not present);
- thiamin (1000×) at 10 mg/mliter.

Considering the microscopic size of EC, the EGFP reservoir is limited. Moreover an EGFP molecule is photodestroyed when $\sim 10^6$ photons are emitted,[19] and a 10-s illumination inexorably blacks out the fluorescence. We therefore increase the reservoir size by adding cephalexin, which allows the bacteria length to grow as large as 100 μm, while maintaining the same diameter (~1 μm). Note that this treatment does not affect EC properties[20] but strongly limits the photobleaching effects.

To increase bacteria length and induce the EGFP expression, we add cephalexin (100 μg/mliter) and IPTG (50 μM), respectively, and incubate for ~30 min. Meanwhile the mirror and the substrate surfaces are coated for 10 min by a 20 μliter droplet of polylysin (0.1 mg/mliter), which helps the EC stick on the surfaces. They are then rinsed with pure water.

To assemble the samples, one with a mirror and one with a substrate, we used home-built chambers. These chambers enable a droplet of EC solution to be squeezed between a conventional microscope cover slide (thickness, ~150 μm and a mirror or a substrate, maintaining a constant liquid spacer of ~80 μm between the two surfaces. These chambers are incubated for 4 h for most of the EC to stick on the polylysin-coated surface.

3. Fluorescence Correlation Spectroscopy Setup

The FCS setup is similar to that previously described.[21] Our custom FCS apparatus is based on a Zeiss Axiovert 200M microscope with a C-Apochromal 40× 1.2 numerical-aperture water-immersion objective (Zeiss, Jena, Germany). The system integrates a piezodriven sample holder (E-710.4CL, Physik Instrumente, Walbronn, Germany) for positioning the excitation volume with nanometric resolutions along all three axes. This positioning is controlled by a homemade program written with Labview (National Instruments, Austin, Tex.). The detection pinhole has a diameter of 50 μm. To avoid after-pulse artifacts, we realize a fluorescence signal cross-correlation by separating light that has just passed through the pinhole on two SPCM-AQR-13 avalanche photodiodes (PerkinElmer Optoelectronics, Dumberry, Canada) connected to an ALV-6010/160 correlator (ALV-GmbH, Langen, Germany). Data are recorded with the correlator software and analyzed by homemade software written with Igor Pro (WaveMetrics, Lake Oswego, Ore.). In front of the detectors we filter the EGFP fluorescence light with narrowband filters that notably reduce background signal.

For the measurements reported here the excitation beam is provided by the 488 nm line of an argon laser cleaned from parasite plasma rays with a narrowband filter. Laser power is attenuated with neutral-density filters and adjusted to underfill the back aperture of the objective.

4. Experimental Autocorrelation Function Acquisition

To perform one Acquisition for one fluorescent species (EGFP or IscS-EGFP), either on a mirror or on a substrate, we set the excitation power to a value ensuring negligible photobleaching (see Subsection 3.C). Before the ACF acquisitions we observed the sample with fluorescence microscopy to choose a well-filamented and well-fastened EC, showing a low EGFP expression due to a small number of diffusing molecules. This enables us to have significant fluorescence fluctuations and not saturate the photodetectors. A fluorescence intensity image is realized in order for us to accurately focus the excitation beam on the EC far from the extremities to avoid edge effects. We record then ~60 ACFs with their associated temporal count rates, each of them for 5 s. We eliminate the ACFs whose temporal count rate presents strong and slow (>1 s) fluctuations. These fluctuations do not result from single-molecule diffusion but possibly from EC undulations or diffusing fluorescent aggregates (see Fig. 8).[22] More than 50% of the ACFs are usually kept and averaged to give one Acquisition.

5. Fluorescence Correlation Spectroscopy in Practice

The general fit function of ACF is given by[11,12]

$$g^{(2)}(\tau) = 1 + (1/N)(\text{noise})(\text{Phot}\varphi)_\tau\, g_x(\tau) g_y(\tau) g_z(\tau), \tag{13}$$

where (noise) and $(\text{Phot}\varphi)_\tau$ are, respectively, a constant correction factor for uncorrelated background intensity and a factor related to intensity fluctuations caused by photophysical properties, such as the population and depopulation of the triplet state.[23,24] $(\text{Phot}\varphi)_\tau$ depends strongly on the environment.[23,25–27]

Since the diffusion modes on the mirror and on the substrate are supposed to be equivalent (see Subsection 3.C), Eq. (10) yields

$$\rho(\tau) = A\left[\frac{(\text{Phot}\varphi)_M}{(\text{Phot}\varphi)_S}\right]_\tau [1 + n_f \exp(-\tau/\tau_f)], \tag{14}$$

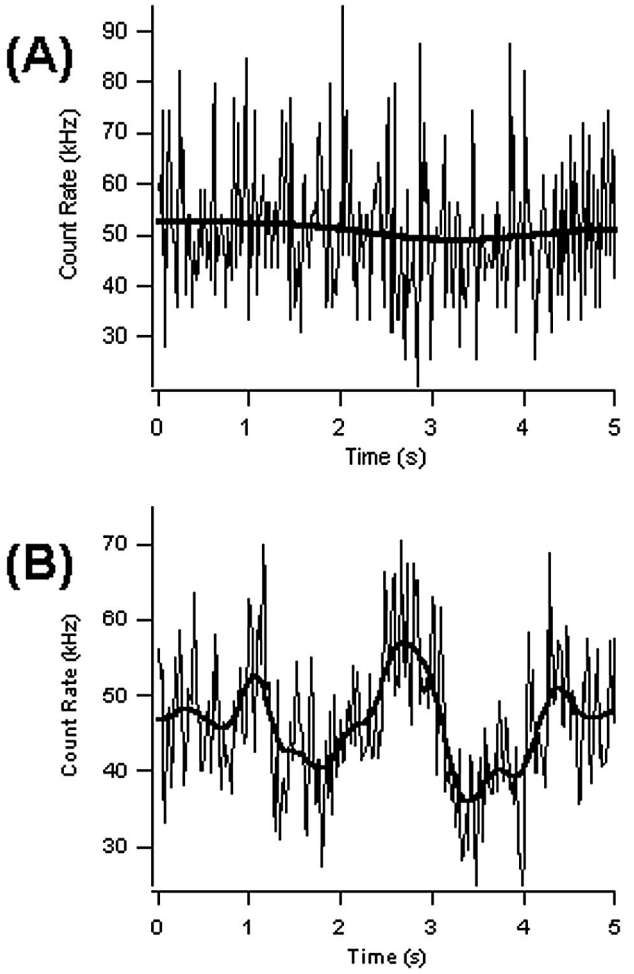

Fig. 8. Examples of temporal count rates obtained in 5 s from EC (light curves) and the quasi-instantaneous average (heavy curves). The ACF associated with the rates in (A) and (B) are, respectively, conserved and excluded from analysis.

where A is a constant given by

$$A = \frac{(\text{noise})_M}{(\text{noise})_S} \frac{N_S}{N_M}. \tag{15}$$

B. Results

We set experimentally the transversal waist to be $\omega_{xy} = 0.45$ μm thanks to a calibration with a Rh6G solution and the excitation power density at $P = 20$ μW before entering the microscope. For a given fluorescent species we first record ~10 Acquisitions for EC on a mirror. We then average these Acquisitions to obtain $\text{ACF}_M(\tau)$. In the case of EC on a substrate we set the excitation power at $2P$ (see Subsection 3.C) and do the same Acquisitions. We obtain $\text{ACF}_S(\tau)$ by averaging. We then calculate the $\rho(\tau)$ function, as described in Eq. (10) and use Eq. (14) for fitting and extracting τ_f. Note that we assumed $(\text{Phot}\varphi)_M = (\text{Phot}\varphi)_S$ (see Subsection 3.C). Figure 9 presents the experimental $\rho(\tau)$ function obtained for IscS-EGFP. The standard deviations are estimated from the Koppel formulation.[17,28] The fringe spacing

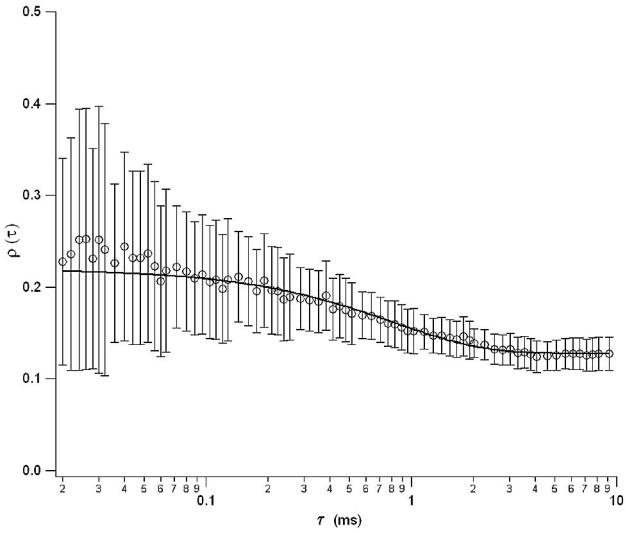

Fig. 9. Experimentally obtained ρ ratio. Circles, ρ ratio obtained from measurements in EC labeled with IscS-EGFP with standard deviations; solid line, fit with Eq. (14) with $(\text{Phot}\varphi)_M = (\text{Phot}\varphi)_S$ ($\omega_{xy} = 450$ nm).

time for IscS-EGFP freely diffusing in EC cytoplasm is found to be $\tau_f^{\text{IscS-EGFP}} = 825 \pm 242$ μs. Thus Eq. (9) leads to the diffusion coefficient $D_f^{\text{IscS-EGFP}} = 1.0 \pm 0.3$ μm^2/s. For EGFP we find $\tau_f^{\text{EGFP}} = 172 \pm 38$ μs, and then $D_f^{\text{EGFP}} = 4.7 \pm 10$ μm^2/s.

C. Discussion

Our measurement of $D_f^{\text{EGFP}} = 4.7 \pm 10$ μm^2/s in EC is in reasonable agreement with the value reported by fluorescence recovery after photobleaching (FRAP) $D_{\text{FRAP}}^{\text{EGFP}} = 7.7 \pm 2.5$ μm^2/s.[20] Although the discrepancy found can be explained by the fact that standard FRAP analysis faces the same problem as standard FCS and probably leads to low-accuracy results, when the observation volume size is comparable with the reservoir size. We emphasize here again that our FCS with a mirror technique permits to measurement of diffusion coefficients in EC without any *a priori* knowledge of the observation volume geometry or the bacteria diameter.[29]

As explained in Subsection 3.B, in the mirror case the excitation power was half of that set in the substrate case. The reflection of the incoming field on the mirror surface enables an average excitation power received per molecule equal in both cases. This allows one to assume that the photophysical properties of the fluorophores are identical in the mirror and substrate cases [$(\text{Phot}\varphi)_M = (\text{Phot}\varphi)_S$], since these molecular parameters and photobleaching are power dependent.[16,23]

In our measurements we found different diffusion coefficients for EGFP and IscS-EGFP that cannot be simply explained by the mass difference between these two proteins diffusing as spherical entities. Indeed, if the proteins diffuse in a medium of constant viscosity η, we would expect (the Stokes–Einstein formula)

$$D = \frac{kT}{6\pi\eta R}, \tag{16}$$

where R is the hydrodynamic radius. Assuming that R scales with the third power of the molecular weight $M^{1/3}$, the ratio of the EGFP diffusion coefficient to that of IscS-EGFP should be

$$\left(\frac{M^{\text{IscS-EGFP}}}{M^{\text{EGFP}}}\right)^{-1/3} \sim 0.7,$$

whereas we experimentally obtained

$$\frac{D_f^{\text{IscS-EGFP}}}{D_f^{\text{EGFP}}} \sim 0.21,$$

with $M^{\text{EGFP}} = 27kDa$ and $M^{\text{IscS-EGFP}} = 75kDa$. An explanation is that interactions increase the effective size of IscS at a constant effective viscosity. However, this leads to a seemingly unreasonably large size for an IscS containing complex of $\sim 3MDa$. The origin of this apparent abnormal size dependence of the diffusion coefficient is a subject of continuing investigation. However, the cytoplasmic molecular congestion can alternatively explain this difference by an apparent viscosity (η^{EGFP} and $\eta^{\text{IscS-EGFP}}$), depending on protein size. We have

$$\frac{\eta^{\text{IscS-EGFP}}}{\eta^{\text{EGFP}}} = \frac{D_f^{\text{EGFP}}}{D_f^{\text{IscS-EGFP}}}\left(\frac{M^{\text{EGFP}}}{M^{\text{IscS-EGFP}}}\right)^{1/3} \sim 3.3.$$

Thus the viscosity seen by the IscS-EGFP complex is 3.3 times higher than the viscosity seen by EGFP. This ratio is in agreement with the previous study, which indicates that cytoplasmic viscosity increases with the protein hydrodynamic radius.[30,31]

4. Conclusion

In this work we have shown that conventional FCS analysis cannot measure accurately the confined diffusion in tubular structures whose diameters are of the order of the confocal volume extension. On the contrary, by using interference fringes that appear on a mirror surface for the excitation field, we have demonstrated that one can accurately measure diffusion coefficients in a tubular structure whose diameter can be as small as $\lambda/2$. Such a measurement is possible because the fringes structure the confocal volume at the $\lambda/2$ scale, providing a new fluctuation time scale on the autocorrelation functions resulting from the diffusion of the fluorophores through the fringes. As soon as the diffusion within one fringe can be considered free (i.e., not sensitive to confinement), one can use this fringe time to deduce the diffusion coefficient in a straightforward manner.

We have applied such a technique to measuring the diffusion coefficient of EGFP tagged proteins diffusing inside *Escherichia coli* cytoplasm and found that the proteins experience different apparent viscosities, depending on their size.

By extending such a concept of optical-field shaping at the subwavelength-scale level, we expect that well-designed photonic structures[32] will allow diffusion to be measured in small cellular compartments.

In Appendices A–C we consider only the fluorescence fluctuations arising from the diffusion of one fluorescent molecule type, neglecting background intensity, photobleaching, and other photophysical processes.

Appendix A: General Theory

Fluctuations in the fluorescence intensity are related to fluctuations in concentration. The fluctuation $\delta C(\mathbf{r}, t)$ of the local concentration $C(\mathbf{r}, t)$ at point $\mathbf{r}$ and time t occurs around the steady-state concentration $\bar{C}$:

$$\delta C(\mathbf{r},\ t) = C(\mathbf{r},\ t) - \bar{C}. \tag{A1}$$

The correlation of the concentration fluctuation $\delta C(\mathbf{r}, t)$ at $\mathbf{r}$ and t with the concentration fluctuation $\delta C(\mathbf{r}', t + \tau)$ at $\mathbf{r}'$ and a later time $t + \tau$ is given by

$$\phi(\mathbf{r},\ \mathbf{r}',\ \tau) = \langle \delta C(\mathbf{r},\ \tau)\delta C(\mathbf{r}',\ t+\tau)\rangle \tag{A2}$$

or assuming stationarity

$$\phi(\mathbf{r},\ \mathbf{r}',\ \tau) = \langle \delta C(\mathbf{r},\ 0)\delta C(\mathbf{r}',\ \tau)\rangle, \tag{A3}$$

where $\langle\ \rangle$ is the ensemble average.[2] The ϕ can be expressed in terms of the probability density for a single molecule that started a random walk at time $\tau = 0$ at point $\mathbf{r}$ to be at $\mathbf{r}'$ at time τ. Thus, because of Fick's second law for diffusion, we have

$$\phi(\mathbf{r},\ \mathbf{r}',\ \tau) = \frac{\bar{C}}{(4\pi D\tau)^{n/2}} \exp\left(-\frac{|\mathbf{r}-\mathbf{r}'|^2}{4D\tau}\right), \tag{A4}$$

where D and n are, respectively, the diffusion coefficient of the considered fluorescent molecules and the dimension number that the fluorescent molecules can explore.

Fluctuations in the fluorescence intensity are detected experimentally as fluctuations in the photocurrent generated in a fluorescence detector. This photocurrent can be written as

$$i(t) = q\int \mathrm{MDE}(\mathbf{r})C(\mathbf{r},\ t)\mathrm{d}\mathbf{r}, \tag{A5}$$

where q is a factor taking into account the absorption and emission cross section of the considered fluorophores, detector gain, and absorption of filters. MDE is the molecular detection efficiency function that is equal to the excitation intensity profile multiplied by the collection efficiency function.

The normalized autocorrelation function of the photocurrent can be defined as

$$g^{(2)}(\tau) = \frac{\langle i(0)i(\tau)\rangle}{\langle i(t)\rangle^2} = 1 + \frac{\langle \delta i(0)\delta i(\tau)\rangle}{\langle i(t)\rangle^2}, \quad \text{(A6)}$$

where

$$\delta i(t) = i(t) - \bar{i} = q \int\int \mathrm{MDE}(\mathbf{r})\delta C(\mathbf{r},\ t)\mathrm{d}\mathbf{r}, \quad \text{(A7)}$$

$$\begin{aligned}\langle \delta i(0)\delta i(\tau)\rangle &= q^2 \int\int \mathrm{MDE}(\mathbf{r})\mathrm{MDE}(\mathbf{r}') \\ &\quad \times \langle \delta C(\mathbf{r},\ 0)\delta C(\mathbf{r}',\ \tau)\rangle \mathrm{d}\mathbf{r}\mathrm{d}\mathbf{r}' \\ &= q^2 \int\int \mathrm{MDE}(\mathbf{r})\mathrm{MDE}(\mathbf{r}') \\ &\quad \times \phi(\mathbf{r},\ \mathbf{r}',\ \tau)\mathrm{d}\mathbf{r}\mathrm{d}\mathbf{r}'. \end{aligned} \quad \text{(A8)}$$

Appendix B: Standard Fluorescence Correlation Spectrocopy Theory

In standard FCS, in the case of the 3D Gaussian approximation of the MDE, we have

$$\mathrm{MDE}(\mathbf{r}) = M_0 \exp\left(-2\,\frac{x^2+y^2}{\omega_{xy}{}^2}\right)\exp\left(-2\,\frac{z^2}{\omega_z{}^2}\right), \quad \text{(B1)}$$

where M_0 is a constant and $\mathbf{r} = (x, y, z)$. The normalized 3D autocorrelation function can also be calculated from Eqs. (A4), (A6), and (B1)[11]:

$$g^{(2)}(\tau) = 1 + (1/N)(1 + \tau/\tau_d)^{-1}\left(1 + s^2\,\tau/\tau_d\right)^{-1/2}, \quad \text{(B2)}$$

where $N = \bar{C}V_d$ with V_d the detection volume defined as

$$V_d = \frac{\left[\int \mathrm{MDE}(\mathbf{r})\mathrm{d}\mathbf{r}\right]^2}{\int [\mathrm{MDE}(\mathbf{r})]^2\mathrm{d}\mathbf{r}}. \quad \text{(B3)}$$

Appendix C: Fluorescence Correlation Spectroscopy on a Mirror Theory

In FCS on a mirror the excitation volume is structured with interference fringes. We have shown in a previous study that the MDE can be well approximated by[15]

$$\mathrm{MDE}(\mathbf{r}) = M_0\,\mathrm{MDE}_x(x)\mathrm{MDE}_y(y)\mathrm{MDE}_z(z), \quad \text{(C1)}$$

with

$$\mathrm{MDE}_j(j) = \exp\left(-\frac{2j^2}{\omega_{xy}{}^2}\right) \quad (j = x,\ y), \quad \text{(C2)}$$

$$\mathrm{MDE}_z(z) = [1 + V\cos(2kz)]\exp\left(-\frac{2z^2}{\omega_z{}^2}\right), \quad \text{(C3)}$$

where $k = 2\pi/\lambda$ and V is the visibility coefficient of the fringes between zero (no fringe) and one (perfect visibility, as in the numerical calculations in this paper). Note that λ stands for the excitation wavelength in the medium where the fluorescent molecules are diffusing.

To derive an analytical form $g^{(2)}(\tau)$ for the autocorrelation function from Eqs. (A4), (A6), and (C1), it is easier to use the Fourier transform. The normalized autocorrelation function can also be written as[33]

$$g^{(2)}(\tau) = 1 + \frac{\int |\mathrm{MDE}(\mathbf{q})|^2\,\phi(\mathbf{q},\ \tau)\mathrm{d}\mathbf{q}}{\underbrace{\int |\mathrm{MDE}(\mathbf{q})|^2\,\phi(\mathbf{q},\ 0)\mathrm{d}\mathbf{q}}_{=\gamma(\tau)}} = 1 + \gamma(\tau), \quad \text{(C4)}$$

where $\mathrm{MDE}(\mathbf{q})$ and $\phi(\mathbf{q}, \tau)$ are the spatial Fourier transforms of $\mathrm{MDE}(\mathbf{r})$ and $\phi(\mathbf{r}, \tau)$, respectively. By definition,

$$\phi(\mathbf{q},\ \tau) = \int \phi(\underbrace{\mathbf{r} - \mathbf{r}'}_{=R},\ \tau)\exp(\mathbf{q}\cdot\mathbf{R})\mathrm{d}\mathbf{R} \quad \text{(C5)}$$

and reciprocally

$$\phi(\mathbf{R},\ \tau) = \frac{1}{2\pi}\int \phi(\mathbf{q},\ \tau)\exp(-i\mathbf{q}\cdot\mathbf{R})\mathrm{d}\mathbf{q}. \quad \text{(C6)}$$

If $\mathbf{q} = (q_x, q_y, q_z)$, we can write

$$\mathrm{MDE}(\mathbf{q}) = M_0\,\mathrm{MDE}_x(q_x)\,\mathrm{MDE}_y(q_y)\,\mathrm{MDE}_z(q_z), \quad \text{(C7)}$$

where

$$\mathrm{MDE}_j(q_j) = \left(\frac{\pi}{2}\right)^{1/2}\omega_{xy}\exp\left(-\frac{q_j{}^2\omega_{xy}{}^2}{8}\right) \quad (j = x,\ y), \quad \text{(C8)}$$

$$\mathrm{MDE}_z(q_z) = \left(\frac{\pi}{2}\right)^{1/2} \omega_z \left\{ \exp\left(-\frac{{q_z}^2 {\omega_z}^2}{8}\right) + \frac{V}{2} \exp\left[-\frac{{\omega_z}^2 (q_z - 2k)^2}{8}\right] + \frac{V}{2} \exp\left[-\frac{{\omega_z}^2 (q_z + 2k)^2}{8}\right] \right\}. \quad \text{(C9)}$$

Moreover, for 3D Brownian diffusion, we have from Eq. (A4):

$$\phi(\mathbf{R}, \tau) = \frac{\bar{C}}{(4\pi D\tau)^{3/2}} \exp\left(-\frac{R^2}{4D\tau}\right) \quad \text{(C10)}$$

So we can write

$$\phi(\mathbf{q}, \tau) = \bar{C}\phi_x(q_x, \tau)\phi_y(q_y, \tau)\phi_z(q_z, \tau) = \bar{C} \exp(-q^2 D\tau), \quad \text{(C11)}$$

where

$$\phi_j(q_j, \tau) = \exp(-{q_j}^2 D\tau) \quad (j = x, y, z). \quad \text{(C12)}$$

Equations (C4), (C7), and (C11) lead to

$$g^{(2)}(\tau) = 1 + \gamma(\tau) = 1 + \gamma_x(\tau)\gamma_y(\tau)\gamma_z(\tau), \quad \text{(C13)}$$

with

$$\gamma_j(\tau) = \frac{\int |\mathrm{MDE}_j(q_j)|^2 \phi_j(q_j, \tau) \mathrm{d}q_j}{\int |\mathrm{MDE}_j(q_j)|^2 \phi_j(q_j, 0) \mathrm{d}q_j} \quad (j = x, y, z). \quad \text{(C14)}$$

From Eqs. (C8) and (C11), we have

$$\gamma_j(\tau) = (1 + \tau/\tau_{d_{xy}})^{-1/2} \quad (j = x, y), \quad \text{(C15)}$$

where $\tau_{d_{xy}} = {\omega_{xy}}^2/4D$.

Concerning $\gamma_z(\tau)$, Eq. (C9) leads to

$$\frac{2}{\pi {\omega_z}^2} |\mathrm{MDE}_z(q_z)|^2 = \frac{V^2}{4} \exp\left[-\frac{{\omega_z}^2 (q_z - 2k)^2}{4}\right] + \frac{V^2}{4} \exp\left[-\frac{{\omega_z}^2 (q_z + 2k)^2}{4}\right] + \exp\left[-\frac{{q_z}^2 {\omega_z}^2}{4}\right] + \frac{V^2}{2} \exp\left[-\frac{{\omega_z}^2 (q_z - 2k)^2}{8} - \frac{{\omega_z}^2 (q_z + 2k)^2}{8}\right] + V \exp\left[-\frac{{\omega_z}^2 (q_z - 2k)^2}{8} - \frac{{q_z}^2 {\omega_z}^2}{8}\right] + V \exp\left[-\frac{{\omega_z}^2 (q_z + 2k)^2}{8} - \frac{{q_z}^2 {\omega_z}^2}{8}\right]. \quad \text{(C16)}$$

However, $\omega_z \gg \lambda$; hence $k\omega_z \gg 1$. In Eq. (C16) we can also neglect the three last terms on the right-hand side.[33] We have

$$\gamma_z(\tau) = \frac{\gamma_1(2k, \tau) + \gamma_1(-2k, \tau) + 4\gamma_1(0, \tau)/V^2}{\gamma_1(2k, 0) + \gamma_1(-2k, 0) + 4\gamma_1(0, 0)/V^2}, \quad \text{(C17)}$$

where

$$\gamma_1(k, \tau) = \int \frac{\pi {\omega_z}^2 V^2}{8} \exp\left[-\frac{{\omega_z}^2}{4}(q_z - k)^2 - {q_z}^2 D\tau\right] \mathrm{d}q_z \quad \text{(C18)}$$

$$= \frac{\pi^{3/2} \omega_z V^2}{4} (1 + \tau/\tau_{d_z})^{-1/2} \times \exp\left[-k^2 D\tau (1 + \tau/\tau_{d_z})^{-1/2}\right], \quad \text{(C19)}$$

with $\tau_{d_z} = {\omega_z}^2/4D$.

From Eqs. (C13), (C15), and (C17), we obtain for a 3D Brownian diffusion

$$g^{(2)}(\tau) = 1 + (1/N)(1 + \tau/\tau_{d_{xy}})^{-1}(1 + \tau/\tau_{d_z})^{-1/2} \times \underbrace{[1 + n_f \exp(-\tau/\tau_f)(1 + \tau/\tau_{d_z})^{-1/2}]}_{\text{fringe factor}}, \quad \text{(C20)}$$

where $n_f = V^2/2$, which agrees with previous studies,[13] and

$$\tau_f = \frac{\lambda^2}{16\pi^2 D}, \quad \text{(C21)}$$

where τ_f is called the fringe spacing time constant and is related to the average time that a particle needs to pass through a bright or a dark fringe.

Since $\tau_f \ll \tau_{d_z}$, for $\tau \simeq \tau_f$ (i.e., $\tau \ll \tau_{d_z}$), the fringe factor related to the diffusion through the fringes can be written $[1 + n_f \exp(-\tau/\tau_f)]$. On the other hand, for $\tau \simeq \tau_{d_z}$ and $\tau > \tau_{d_z}$, the fringe factor tends toward 1 as $[1 + n_f \exp(-\tau/\tau_f)]$. Thus we can consider an approximate form for Eq. (C20):

$$g^{(2)}(\tau) \simeq 1 + \frac{1}{N}(1 + \tau/\tau_{d_{xy}})^{-1}(1 + \tau/\tau_{d_z})^{-1/2} \times [1 + n_f \exp(-\tau/\tau_f)], \quad \text{(C22)}$$

Equation (C21) indicates that this fringe spacing time does not depend on transversal waist ω_{xy}.[13] Thus fitting the ACF resulting from FCS on a mirror allows diffusion coefficient measurements without *a priori* knowledge of the detection volume geometry and only because of knowledge of the excitation beam wavelength.[14]

Note that N in Eq. (C20) and approximation (C22) is the total number of fluorescent molecules present in the detection volume without fringes. If N' is the total number of fluorescent molecules present in the detection volume with fringes, we have

$$N = \frac{V^2 + 2}{2} N' = (1 + n_f)N'. \quad \text{(C23)}$$

The authors thank M. Cathelinaud for manufacturing the mirrors.

References

1. D. Magde, E. L. Elson, and W. W. Webb, "Thermodynamic fluctuations in a reacting system measurement by fluorescence correlation spectroscopy," Phys. Rev. Lett. **29,** 705–708 (1972).
2. E. L. Elson and D. Magde, "Fluorescence correlation spectroscopy. 1. Conceptual basis and theory," Biopolymers **13,** 1–27 (1974).
3. D. Magde, E. L. Elson, and W. W. Webb, "Fluorescence correlation spectroscopy. 2. An experimental realization," Biopolymers **13,** 29–61 (1974).
4. R. Rigler, U. Mets, J. Widengren, and P. Kask, "Fluorescence correlation spectroscopy with high count rate and low background: analysis of translational diffusion," Eur. Biophys. J. **22,** 169–175 (1993).
5. S. T. Hess and W. W. Webb, "Focal volume optics and experimental artifacts in confocal fluorescence correlation spectroscopy," Biophys. J. **83,** 2300–2317 (2002).
6. P. Schwille, U. Haupts, S. Maiti, and W. W. Webb, "Molecular dynamics in living cells observed by fluorescence correlation spectroscopy with one- and two-photon excitation," Biophys. J. **77,** 2251–2265 (1999).
7. P. Schwille, J. Korlach, and W. W. Webb, "Fluorescence correlation spectroscopy with single-molecule sensitivity on cell and model membranes," Cytometry **36,** 176–182 (1999).
8. J. C. Politz, E. S. Browne, D. E. Wolf, and T. Pederson, "Intramolecular diffusion and hybridization state of oligonucleotides measured by fluorescence spectroscopy in living cells," Proc. Natl. Acad. Sci. USA **95,** 6043–6048 (1998).
9. M. Wachsmuth, W. Waldeck, and J. Langowski, "Anomalous diffusion of fluorescent probes inside living cell nuclei investigated by spatially resolved fluorescence correlation spectroscopy," J. Mol. Biol. **298,** 677–689 (2000).
10. P.-F. Lenne, D. Colombo, H. Giovannini, and H. Rigneault, "Flow profiles and directionnality in microcapillaries measured by fluorescence correlation spectroscopy," Single Mol. **3,** 194–200 (2002).
11. S. R. Aragon and R. Pecora, "Fluorescence correlation spectroscopy as a probe of molecular dynamics," J. Chem. Phys. **64,** 1791–1803 (1976).
12. A. Gennerich and D. Schild, "Fluorescence correlation spectroscopy in small cytosolic compartments depends critically on the diffusion model used," Biophys. J. **79,** 3294–3306 (2000).
13. H. Asaï and T. Ando, "Fluorescence correlation spectroscopy illuminated by standing exciting light waves," J. Phys. Soc. Jpn. **40,** 1527–1528 (1976).
14. P.-F. Lenne, E. Etienne, and H. Rigneault, "Subwavelength patterns and high detection efficiency in fluorescence correlation spectroscopy using photonic structures," Appl. Phys. Lett. **80,** 4106–4108 (2002).
15. H. Rigneault and P.-F. Lenne, "Fluorescence correlation spectroscopy on mirror," J. Opt. Soc. Am. **20,** 2203–2214 (2003).
16. J. Wiaengren and R. Rigler, "Mechanisms of photobleaching investigated by fluorescence correlation spectroscopy, Bioimaging **4,** 149–157 (1996).
17. T. Wohland, R. Rigler, and H. Vogel, "The standard deviation in fluorescence correlation spectroscopy," Biophys. J. **80,** 2987–2999 (2001).
18. B. V. Bronk, S. D. Druger, J. Czg, and W. P. Van De Merwe, "Measuring diameters of rod-shaped bacteria *in vivo* with polarized light scattering," Biophys. J. **69,** 1170–1177 (1995).
19. A. Zumbusch and G. Jung, "Single molecule spectroscopy of the green fluorescent protein: a critical assessment," Single Mol. **1,** 261–270 (2000).
20. M. B. Elowitz, M. G. Surette, P.-E. Wolf, J. B. Stock, and S. Leibler, "Protein mobility in the cytoplasm of *Escherichia coli,*" J. Bacteriol. **181,** 197–203 (1999).
21. L. Wawrezinieck, H. Rigneault, D. Marguet, and P.-F. Lenne, "Fluorescence correlation spectroscopy diffusion laws to probe the submicrometer cell membrane organization," Biophys. J. **89,** 4029–4042 (2005).
22. K. Bacia and P. Schwille, "A dynamic view of cellular processes by *in vivo* fluorescence autocorrelation and cross-correlation spectroscopy," Methods **29,** 74–85 (2003).
23. J. Widengren, R. Rigler, and U. Mets, "Triplet-state monitoring by fluorescence correlation spectroscopy," J. Fluoresc. **4,** 255–258 (1994).
24. J. Widengren, U. Mets, and R. Rigler, "Fluorescence correlation spectroscopy of triplet states in solution: a theoretical and experimental study," J. Phys. Chem. **99,** 13368–13379 (1995).
25. J. Widengren and P. Schwille, "Characterization of photoinduced isomerization and back-isomerization of the cyanine dye cy5 by fluorescence correlation spectroscopy," J. Phys. Chem. **104,** 6416–6428 (2000).
26. K. Suhling, J. Siegel, D. Phillips, P. M. W. French, S. Lvque-Fort, S. E. D. Webb, and D. M. Davis, "Imaging the environment of green fluorescent protein," Biophys. J. **83,** 3589–3595 (2002).
27. U. Haupts, S. Maiti, P. Schwille, and W. W. Webb, "Dynamics of fluorescence fluctuations in green fluorescent protein observed by fluorescence correlation spectroscopy," Proc. Natl. Acad. Sci. USA **95,** 13573–13578 (1998).
28. D. E. Koppel, D. Axelrod, J. Schlessinger, E. L. Elson, and W. W. Webb, "Dynamics of fluorescence marker concentration as probe of mobility," Biophys. J. **16,** 1315–1329 (1976).
29. I. Ventre, F. Ledgham, V. Prima, A. Lazdunski, M. Foglino, and J. N. Sturgis, "Dimerization of the quorum sensing regulator RhlR: development of a method using EGFP fluorescence anisotropy," Mol. Microbiol. **48,** 187–198 (2003).
30. M. Arrio-Dupont, S. Cribier, G. Foucault, P. F. Devaux, and A. d'Albis, "Diffusion of fluorescently labeled macromolecules in cultured muscle cells," Biophys. J. **70,** 2327–2332 (1996).
31. M. Arrio-Dupont, G. Foucault, M. Vacher, P. F. Devaux, and S. Cribier, "Translational diffusion of globular proteins in the cytoplasm of cultured muscle cells," Biophys. J. **78,** 901–907 (2000).
32. H. Rigneault, J. Capoulade, J. Dintinger, J. Wenger, N. Bonod, E. Popov, T. W. Ebbesen, and P.-F. Lenne, "Enhancement of single molecule fluorescence detection in subwavelength apertures," Phys. Rev. Lett. **95,** 117401–117404 (2005).
33. T. Sonehara, K. Kojima, and T. Irie, "Fluorescence correlation spectroscopy excited with a stationary interference pattern for capillary electrophoresis," Anal. Chem. **74,** 5121–5131 (2002).